ELSEVIER

Organic photovoltaics: Crosslinking for optimal morphology and stability

Joseph W. Rumer[1,*] and Iain McCulloch[1,2]

[1] Department of Chemistry and Centre for Plastic Electronics, Imperial College London, London SW7 2AZ, UK
[2] Physical Sciences and Engineering Division and SPERC, King Abdullah University of Science and Technology (KAUST), Thuwal 23955-6900, Saudi Arabia

Organic solar cells now exceed 10% efficiency igniting interest not only in the fundamental molecular design of the photoactive semiconducting materials, but also in overlapping fields such as green chemistry, large-scale processing and thin film stability. For these devices to be commercially useful, they must have lifetimes in excess of 10 years. One source of potential instability, is that the two bicontinuous phases of electron donor and acceptor materials in the photoactive thin film bulk heterojunction, change in dimensions over time. Photocrosslinking of the π-conjugated semiconducting donor polymers allows the thin film morphology to be 'locked' affording patterned and stable blends with suppressed fullerene acceptor crystallization. This article reviews the performance of crosslinkable polymers, fullerenes and additives used to-date, identifying the most promising.

Introduction

Since the award of a Nobel Prize in Chemistry in 2000 for "*the discovery and development of conductive polymers*" [1] organic electronic materials are emerging in applications such as mobile phone displays and niche products such as laptop bags with built-in solar powered chargers [2]. Additional potential applications include solid-state lighting, thermoelectrics and lasers, with prospective applications in textiles, construction and health care [3]. For example, BASF have recently developed a concept car with Daimler, incorporating a transparent organic solar cell in the roof [4]. The potential of organic electronics rests not in their inherently inexpensive composition – being based largely on the earth's most abundant elements: carbon, nitrogen and oxygen – but rather in their amenability to solution processed manufacturing methods, such as ink-jet and roll-to-roll (R2R) printing [5–7]. Inherent to R2R printing is flexibility, light-weight and large-scale compatibility. This makes for a contrast to rigid, more fragile and inherently small-area, batch-produced, inorganic solar cells, cut from crystalline silicon [2]. Coupled with a shortage of fossil fuels and rising carbon dioxide levels, a growing global energy demand makes solar an underexploited renewable energy source. Organic solar cell devices are an emerging class of photovoltaics, but have up until this point been unable to both overcome up-scaling challenges and find an appropriate market entry application. However, the superior performance of organic solar cell devices to inorganics such as silicon for indoor applications, coupled with the need for ubiquitous low energy indoor wireless transmission devices, offers a genuinely unique opportunity for organic photovoltaics as a light harvesting product and it is essential to ensure that this product offering is robust and comprehensive. It is often cited that successful commercialization of solution deposited organic solar cells will rely on the combination of performance, lifetime and cost simultaneously achieving appropriate values. A target of 10% power conversion efficiency (PCE) is generally accepted for organic solar modules, or photovoltaic (OPV) devices, to become commercially viable [8], which has now been surpassed at the research level [9–11]. The new challenge for the OPV community is to deliver high performance combined with sufficient long-term stability, with a generally accepted target being a lifetime of 10 years [12,13]. Whilst it is a simple task to track performance increases in the field, improvements in both lifetime and cost are less easy to measure or track. Much more effort will be focused on these parameters as development and production commences. Avoidance of low yielding, complicated and multi-step synthesis with expensive

*Corresponding author. Rumer, J.W. (jwrumer@imperial.ac.uk), McCulloch, I. (i.mcculloch@imperial.ac.uk)

 http://dx.doi.org/10.1016/j.mattod.2015.04.001

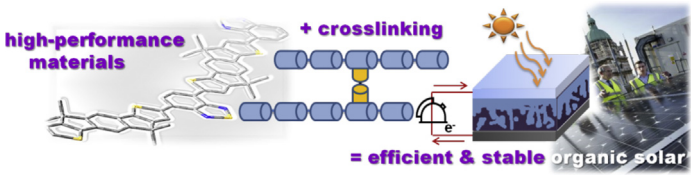

FIGURE 1

Organic crosslinking high performance materials with a defined morphology may afford efficient and stable organic photovoltaic cells.

reagents will become more imperative, and the use of ''universal'' crosslinking additives is a step forward to address both cost and lifetime (Fig. 1).

The four main types of solar cell device instability are thermal (heat), photo (light), chemical (atmosphere) and mechanical (bending and shock). These are likely to be variable in intensity, for example temperature cycling through day and night. While intrinsic material stability is desirable, device encapsulation for example can provide a solution to oxidative and photo instabilities [14]. Device stability is governed by the choice of photoactive layer, interlayers and electrode composition, with experimental measurement conditions such as light exposure, temperature, pre-evaluation annealing and atmosphere (ambient or inert) also influencing results. However, stability testing is becoming more standardized as the field progresses, with accelerated ageing, life-cycle and outdoor testing [15].

Basic OPV device structure consists of a photoactive layer comprising a blend of light absorbing electron donor and acceptor materials sandwiched between two electrodes, one of which is required to be at least semi-transparent. A number of special reviews explaining the device physics and operation have recently been published [16–18] with the key principles being illustrated in Fig. 2. Power conversion efficiency (PCE, η) is the ratio of the maximum power point (P_m) to the input power (P_{in}), the latter being the product of light irradiance (E, W/m^2) and cell surface area (A_c, m^2) under standard test conditions.[3] The maximum power point (P_m) is the product of the cell's internal properties: current (short-circuit current: J_{sc}), photovoltage (open-circuit voltage: V_{oc}) and fill factor (FF). When the photoactive layer absorbs light, donor electrons are promoted from the valence to the conduction band (the energy difference being termed the 'band-gap'). This leaves behind positively charged, Coulombically bound holes, the pair being termed an exciton. Before decay to the ground state, excitons may diffuse through a conjugated structure. Should the exciton meet an acceptor interface, charge separation can occur: the electron drops to the lower energy conduction band, breaking the exciton. At this point there are a variety of mechanisms of recombination, delocalization and charge separation, the latter of which is required to generate free charge carriers which can then transport to their respective electrodes generating a current.

On a molecular design level, the principle requirement of an organic semiconductor is a π-conjugated system of alternating (delocalized) saturated and unsaturated bonds, typically comprising planar aromatic units with delocalized frontier molecular orbitals. A rigid-rod like polymer backbone, with large macromolecular chains assembled from smaller repeat units termed monomers is required. These units are designed to have a certain structural shape and interactions, to achieve desired levels of solubility, absorption of sunlight, charge generation and transport [19].

Low bandgap materials are popular electron donors as their absorption optimally matches the solar spectrum, often resulting in increased charge generation and short-circuit current when compared with wider bandgap polymers (*i.e.* greater than 1.5 eV). In addition, when the material is in the neutral state, a low lying valence band – or highest occupied molecular orbital (HOMO) – can confer intrinsic stability to atmospheric dopants such as oxygen and water. However, the microstructure of the blend is critical in achieving high efficiency, the most common being the bulk heterojunction (BHJ): an inter-percolating thin film structure of both donor and acceptor materials between the electrodes, with domains ideally within exciton diffusion length scale (~10 nm) to avoid exciton decay. While the most studied OPV system has been a BHJ blend of the polymer poly(3-hexylthiophene-2,5-diyl) (**P3HT**) and **PC60BM** fullerene ([6,6]-phenyl C60-butyric acid methyl ester), surpassing 5% PCE with optimal processing [20–22], a number of novel materials have now exceeded 8.5% PCE in BHJ-based photoactive layers with optimized processing (Fig. 3), such as **PTB7** yielding up to 9.2% PCE [23] and recently synthesized **PTB7-Th** yielding up to 11.1% PCE [24]. Other benzodithiophene materials include **PBF100** (8.8%) [25], **PBDTTPD** (8.5% PCE) [26], and **PBDT-DTNT** (8.6%) [27]. A polymer which enables high fill-factor (76%) **PBTI3T** has achieved 8.7% PCE [28] and **PIDTT-DFBT** 8.6% [29]. In addition, the popular **DPP**-motif can afford 8.5% PCE [30]. Most recently polymers **PffBT4T-2OD**, **PBTff4T-2OD** and **PNT4T-2OD** were recently reported with PCEs as high as 10.8%, 10.4% and 10.1% [31].

High performance has also been obtained from multi-junction devices [32], comprising fullerenes in layers such as **PMDPP3T/PCDTBT** (9.6% PCE) [33], **PBDTT-DPP/P3HT** (8.8%) [34,35], **PBDTT-SeDPP/P3HT** (9.5%) [36], **PBDTP-DPP/P3HT** (8.5%) [35], **PBDTFBZS/PNDTDPP** (9.4%) [37] and **PDTP-DFBT/P3HT**, which gave 10.6% PCE [38,39].

Noteworthy to mention – whilst beyond the scope of this review – small molecules [40,41], all-polymer photoactive layers [42], block copolymers [43] and non-fullerene acceptors [44–46] have also been used to fabricate high-performance OPV cells, with >8% PCE being observed in an additive-free non-annealed **BBTI** polymer-based device [47].

Meanwhile, the intrinsic stability of donor polymers in particular has been enhanced by incorporating electronegative heteroatoms to lower the energy of the HOMO and LUMO levels by lowering the electron density in the conjugated system. Materials derived from natural dye pigments have also attracted much attention, exhibiting both high-performance and innate stability [48].

Understanding the influence of molecular design and ordering on the stability of device microstructures has been critical in achieving the highest performance from the active materials [49]. Crystalline materials allow for strong solid-state interactions between conjugated polymer backbones, such as π–π stacking, enhancing charge carrier mobility in OFETs and potentially

[3] Standard test conditions: temperature = 25 °C, irradiance = 1000 W/m^2, air mass = 1.5 (AM1.5 spectrum).

$$PCE = \eta = \frac{P_m}{P_{in}} = \frac{V_{oc} \cdot J_{sc} \cdot FF}{E \cdot A_c}$$

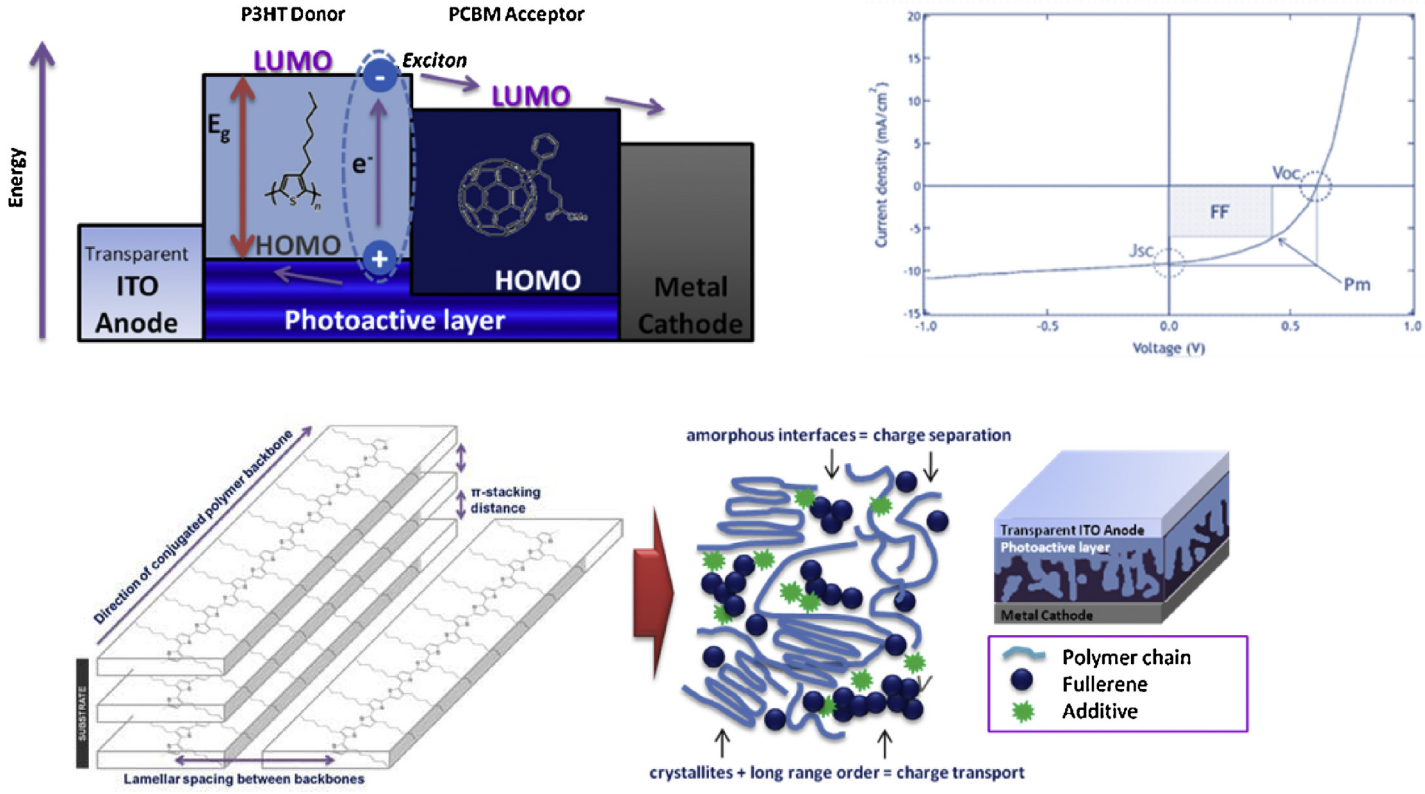

FIGURE 2

Organic photovoltaic principles: (*top left*) the bulk heterojunction device architecture showing **P3HT** donor polymer and **PCBM** fullerene acceptor structures; (*top right*) a typical current–voltage curve illustrating OPV parameters; (*bottom left*) solid-state lamellar packing and π-stacking of crystalline planar conjugated polymers (**rrP3HT** shown in example); and (*bottom right*) the desired microstructure of crystallites and amorphous regions with long-range order in a bulk heterojunction blend, often induced by additive processing.

long-term stability in BHJs through resistance to fullerene diffusion and crystallization. However, sufficient mixing between the donor polymer and fullerene acceptor is also required for efficient charge separation, with the importance of both fullerene and polymer crystallite regions for charge transport, in addition to dispersed amorphous phases for charge generation recently being demonstrated [50].

The development of silicon mould nano-imprinting processes allows for precise control over the nanostructure; for example **TDPTD** patterned with feature sizes below 10 nm leads to a precisely interdigitated active layer in the range of the exciton diffusion lengths, more than tripling PCE [51]. Likewise thermally crosslinkable hole conducting tetraphenylbenzidene small molecules have been prepared and used to produce free-standing nanorod arrays [52] and well-ordered BHJ microstructures [53]. The use of additives to promote ordering has also been studied (Fig. 2). A few volume percentage by weight of 1,8-diiodooctane in a blend of **PCPDTBT**[4]**:PC70BM** red-shifted the absorption, improving PCE by 1.7% (from 3.4% to 5.1%) due to greater chain interactions and improved local structure [54]. Thermal annealing has also been shown to improve active layer morphology with the development of vibronic structure, red-shifting absorption to increase light harvesting and improving electrode contacts: **P3HT:PC60BM** blends have increased by over 2.5% PCE when heated at 150°C for 10 min [55].

Processing attempts to control morphology have previously included phase separation of block copolymers, patterning with anodic alumina templates and self-organization of nanocrystals in polymer brushes [56–58], silicon mould nanoimprinting [51], use of additives to promote ordering [54] and thermal annealing [55]. However, once optimized, the microstructure must be stable over time, exhibiting resistance to thermal, chemical and photo-degradation. The optimized solar cell is a culmination of optimal molecular structure, morphological control and device fabrication technique and architecture.

Strategies for long-term stability include 'locking' the morphology by crosslinking, producing inherently stable materials and encapsulation [59]. Encapsulation should reduce water penetration to levels of less than 10^{-3} g/(m^2 day) [60] and be compatible with roll-to-roll processes: current barriers include inorganics such

[4] Poly[2,6-(4,4-bis-(2-ethylhexyl)-4*H*-cyclopenta[2,1-b;3,4-b′]-dithiophene)-*alt*-4,7-(2,1,3-benzothiadiazole)].

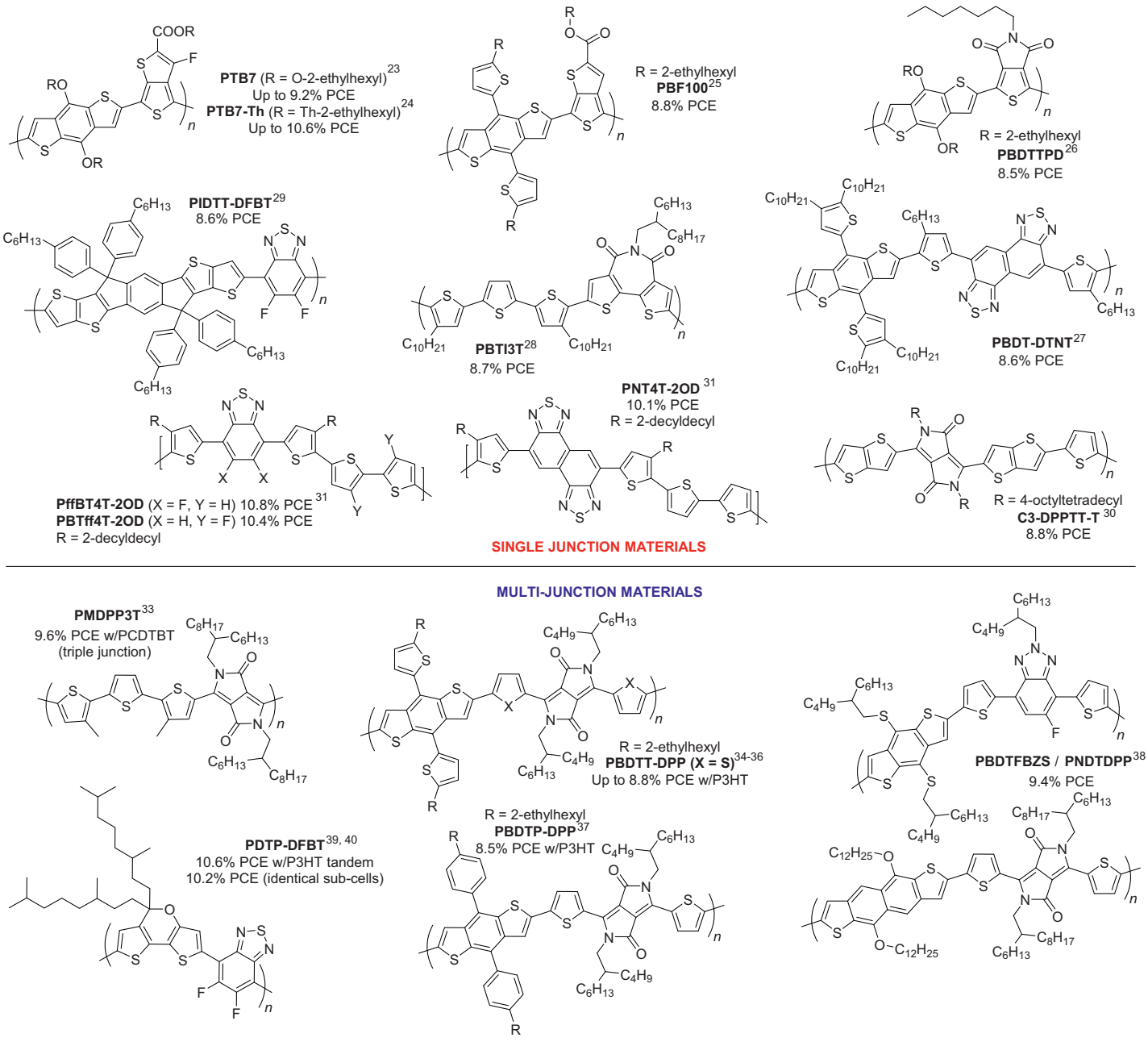

FIGURE 3

OPV materials giving over 8.5% PCE in single and multi-junction devices (all PCEs are maximum values obtained).

as silicon and aluminium oxide, organics and more recently hybrids and multi-layers, though further work is still required to find an optimal material, especially where transparency is required [14].

Crosslinkable polymers to control bulk heterojunction morphology

Recently attention has focused on crosslinking (Fig. 4), incorporating crosslinkable groups on electron donor materials [61], acceptors [62] and small molecules that are added to the photoactive layer blend [63]. The functionalities used to-date include oxetane [64], bromo [65], vinyl [66] and azide [67] functional groups. These have the feature of being amenable to activation either thermally, or more preferably in photochemical processes which do not perturb blend morphologies, such as exposure to deep UV light (DUV) for a specified time period. The crosslinking group, when affixed to a polymer, has been typically located at the solubilizing alkyl side-chain termini on a fixed portion of copolymers (the distribution of which along the polymer backbone has been often random) facilitating crosslinking without severely disrupting the polymer backbone π–π stacking.

Most recently the photo-dimerization of fullerenes by visible light has been shown to stabilize the bulk heterojunction morphology (with a range of donor polymers) [68]. Whilst elevated temperatures (>100°C) lead to scission of the photo-dimerised species, this highlights the importance of thermal ageing in the presence of light to obtain a more accurate picture of morphological change. This phenomenon is attributed to reduced diffusion of

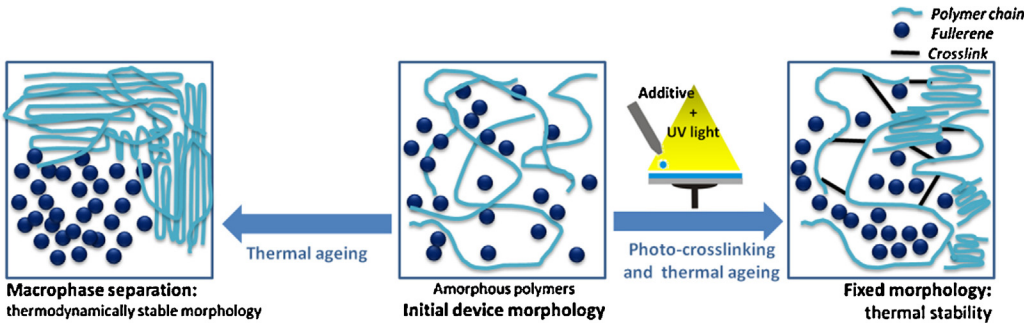

FIGURE 4

Additive crosslinking conveys thermal stability to optimized blends inhibiting macrophase crystallization (shown here for a portion of the substrate).

the fullerenes and resultantly suppressed crystallization, the dimerization being evidenced by Raman spectroscopy and GPC analysis. Furthermore a simple light exposure step can be added to stabilize, and in some cases enhance, device performance [69].

Laboratory photocrosslinking is often carried out with low power handheld UV lamps under an inert atmosphere (nitrogen or argon), in the deep UV wavelength range (~254 nm) with curing times ranging from a few seconds to thirty minutes or longer, in many cases followed by 'soft-curing' (low-temperature, thermal annealing) (Table 1). The oxetane functionality is useful as it is readily crosslinked with a photoacid initiator and UV light *via* a ring opening process. However, the addition of such initiators can be problematic, forming cations with several possible reaction pathways which could be detrimental to device performance [70]. Meanwhile, the bromo-based crosslinking likely occurs *via* a non-selective radical mechanism, which may be disadvantageous as the bromine radicals produced could have a negative impact on device performance and long-term stability. In contrast, no additives are required or side products produced with vinyl crosslinking, which occurs *via* a simple [2+2] cycloaddition. Additionally, the chemistry does not generate polar functional groups, which are capable of acting as charge traps. Similarly the azide functionality does not require an initiator or produce radicals, instead emitting inert nitrogen gas and forming a highly reactive nitrene, capable of insertion and addition reactions.

The majority of crosslinking functionalities have been exemplified using alkyl thiophene backbones (see Fig. 5); in each case the polymers are assumed to be of comparable molecular weight and solubility with optical and electronic properties significantly unchanged. The bromo derivative of P3HT [poly(3-hexylthiophene-2,5-diyl)] **P3HT-Br** has been studied in depth [65], retaining ~90% of initial PCE on ageing. Varying the Br fraction between 5, 10 and 20% has no significant effect on as-made device performance, though crosslinking by DUV reduced the initial PCE from ~2.9 to 2.6%. However, after annealing at 150°C for 48 h, PCE remained at 2.3%, implying greater stability, with polythiophene stacking unaffected and no **PCBM** crystallites visible by grazing incidence wide-angle X-ray scattering after 24 h of annealing, in contrast to micron sized crystallites in the non-crosslinked devices. Current, voltage and fill-factor characteristics were unchanged. Similarly, the vinyl derivative **P3HNT** (poly(-3-(5-hexenyl)thiophene)) has been shown to exhibit similar morphological properties to **P3HT** with improved device stability (using 100% vinyl-functionalized monomers) [66]. In this case, as-made device performance was essentially the same as **P3HT**, though on ageing the PCE retained only ~60% of its initial value (compared to ~90% for **P3HT-Br**), the system thus being considerably less stable under this ageing regime. Similarly the azide derivative, **P3HT-N5** (5% functionalized monomers) retained only ~65% of PCE under a comparatively mild ageing regime (40 h at 110°C), despite optical microscopy showing inhibition of fullerene aggregation [67]. Moreover, an initial PCE 0.5% lower than the reference offsets the benefit of stabilization in the system. This is attributed to the reduced as-made short-circuit current, possibly arising from a compromised morphology, limiting charge separation, or photochemical degradation due to the harsh crosslinking conditions employed (60 min UV exposure in air). In contrast, oxetane functionalized **P3HT** has not been prepared to-date, though polythiophenes **PTHOT** and **PTHOBT** have been synthesized, with 100% of the alkyl side-chains being functionalized [64]. Advantageously the polymers were processable from environmentally benign solvents such as ethanol, whilst being insoluble upon photocrosslinking in the presence of an initiator. Patterned OFETs were prepared with good hole mobilities, reasonable on/off ratios and low threshold voltages. Polythiophene-based OFETs have also been prepared with a self-assembled nanowire fibril morphology which can be crosslinked by virtue of thiol groups at the end of the alkyl side-chains [71]. This approach is particularly interesting due to the reversible nature of the crosslinking, while the structure and charge carrier mobility of the nanowires show no significant change.

A systematic study of the four photocrosslinkable functionalities has also been conducted for the low band gap polymer **TQ1**

TABLE 1

Crosslinking functionalities used in organic photovoltaic materials.

Functionality	Activation	Comments
Oxetane	1. Addition of photo acid generator	Requires PAG additive
	2. UV light exposure	
	3. Typical further soft-curing	Generates radical cations/trap states, requiring neutralization
	4. Neutralization and drying	
Bromo	1. UV light exposure	Generates bromine radicals
Vinyl	2. Optional further 'soft-curing'	Reversible at high temperatures
Azide		Generates inert nitrogen gas

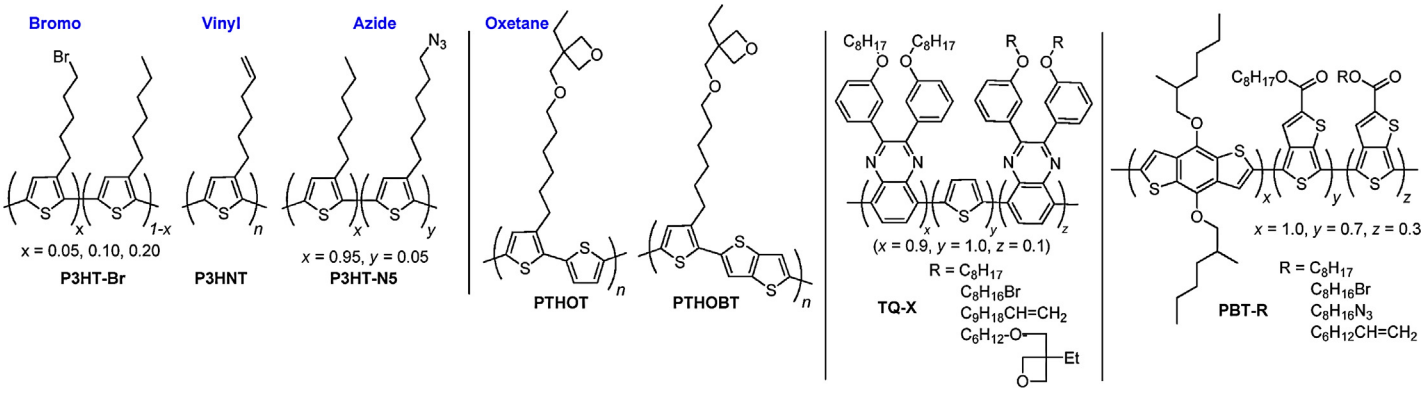

FIGURE 5

Crosslinkable **P3HT**, **TQ** and **PBT** polymer derivatives.

[72] and for all but oxetane for **PBT-R** [73], a derivative of the high performing polymer **PTB-7** (Fig. 5) [74]. In the case of **TQ1**, each polymer was prepared with 10% of alkyl side-chains being functionalized. Notably all four polymers exhibited similar photochemical stability to the reference polymer, **TQ1**, investigated by plotting normalized absorption *versus* irradiation time under constant illumination (AM1.5G, 1000 W m^{-2}). This implied that stability enhancement associated with crosslinking has a thermal origin, such as suppressing morphological changes (namely fullerene aggregation), which was again confirmed by optical microscopy before and after thermal annealing. However, when device stability was then measured under a variety of ageing regimes (100°C; dark *versus* light and ambient *versus* inert atmosphere) there was no consistent trend between polymer stability and crosslinking functionality, with PCE dropping to less than 60% of the initial value in all cases. The detailed analysis is critical in unambiguously establishing photochemical degradation as the primary factor responsible for instability in the **TQ1**:**PCBM** system.

In comparison, for the case of three **PBT-R** polymers (15% functionalized monomers; Fig. 5), all exhibited unchanged as-made properties. Photocrosslinking UV exposure was optimized to 20 min (judged by film insolubility) but 30 min used to ensure completeness. By optical microscopy, fullerene aggregation is suppressed according to the order: bromo > azide > vinyl ≫ refer- reference. The stabilization of PCE followed the same trend, with

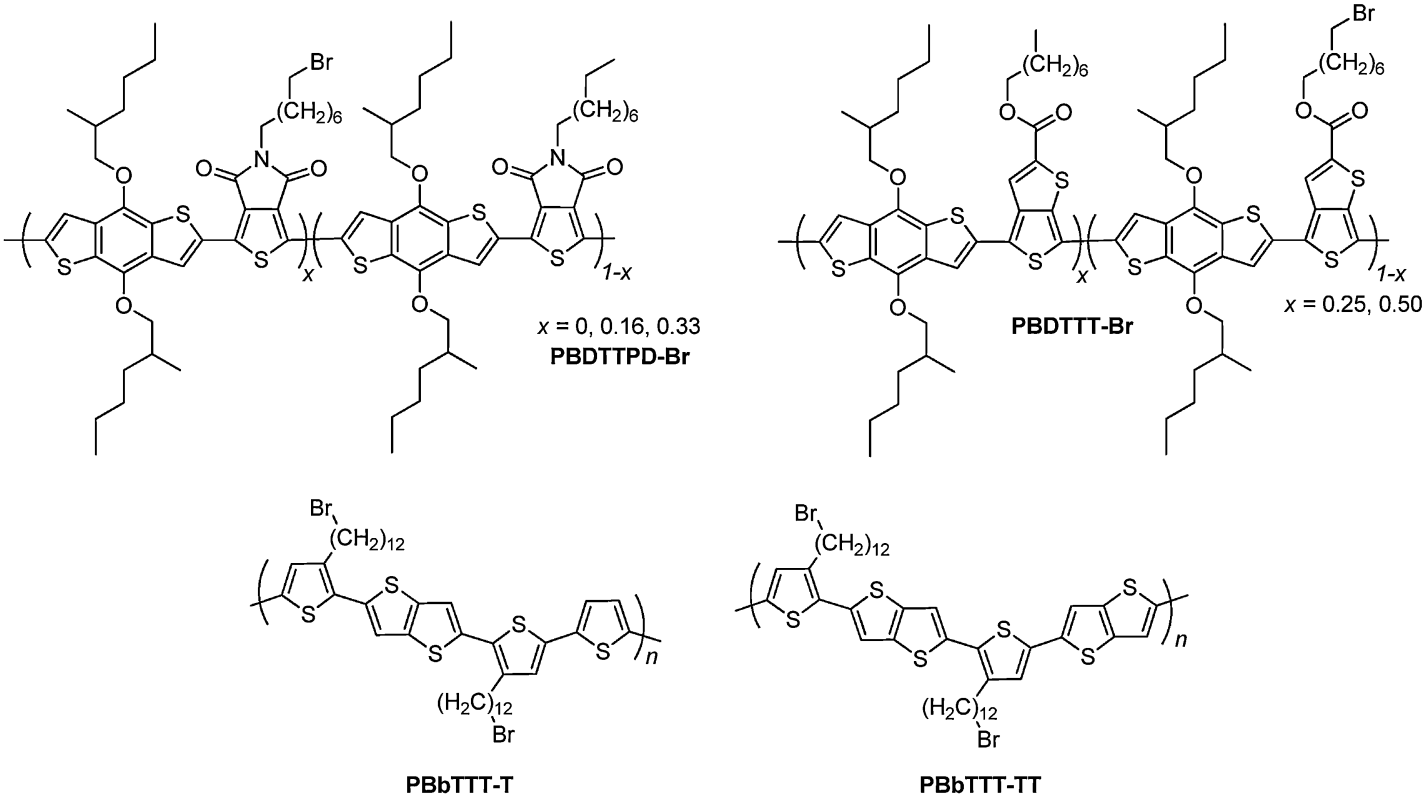

FIGURE 6

Crosslinkable (electron donor) semiconducting polymers.

~80% of PCE being retained for **PBT-Br** after ageing (150°C, 80 h), representing excellent stability without compromising as-made performance.

The first crosslinkable push-pull type electron donor polymer reported in the literature was **PBDTTPD-Br** which exhibited good long-term thermal stability [61]. Polymers functionalized with bromine on 16% of the **TPD** *N*-alkyl side-chains gave the highest performance, with average PCE increasing on ageing (annealing at 150°C for 72 h) from 3.3% to 4.6%, while the reference cell dropped from 5.2% to 3.9%. The increase in PCE of the crosslinked cell is attributed to preservation of short-circuit current, achieved by morphological stabilization on the aggregation scale, combined with an increase in open-circuit voltage – which may be attributed to a change in energy of the interfacial charge-transfer states between the polymer and fullerene components – and an 18% increase in FF.

In addition to **PBT-R** and **PBDTTPD-Br** polymers, bromo-functionalized **PBDTTT** polymers have also been prepared (25% or 50% brominated TT alkyl side-chains; Fig. 6). UV exposure time was investigated showing little difference in film retention (on spin-washing) between 10 and 30 min, but reduced retention after just 5 min. On annealing the Br-25% device PCE plateaued after eight hours, retaining ~65% of initial PCE, with fullerene aggregation being suppressed. More noteworthy and akin to that aforementioned, initial PCE improved on crosslinking by almost 1% from 4.3% to 5.2% [75].

In addition, the liquid-crystalline polymer **PBbTTT-T** and its analogue **PBbTTT-TT** have also been prepared (Fig. 6). The spaced dodecyl alkyl side-chains (100% bromine functionalized) permit the intercalation of fullerenes that can then be 'locked' in place *via* crosslinking, the films then becoming insoluble in dichlorobenzene (ODCB). After optimization of the blend ratios a PCE of 2.6% was achieved for 1:3.5 wt **PBbTTT-TT:$PC_{71}BM$**, dropping slightly to 2.4% on ageing (150°C, 40 h) [76].

Crosslinkable small molecule additives

A fundamentally different and versatile strategy is the addition of small molecule crosslinkers to the photoactive layer blend: ideally a very low concentration of crosslinker could be added to any blend, being activated in a scalable process (such as photocrosslinking), free from potentially detrimental by-products. Recently developed sterically hindered fluoro-phenyl-azides (**sFPA**'s) [77] have been used to crosslink **F8BT**, **PFB**, **TFB** and **OC_1C_{10}-PPV** polymers. Exposure to DUV generates a singlet nitrogen species which then inserts into C–H bonds at alkyl chain termini, directed by the isopropyl steric group. Less than 1 mol% of crosslinker was required for high molecular mass polymers, with a near perfect >0.9 links per crosslinker molecule and no observed quenching of photoluminescence efficiency or reduction of current. **sFPA** has also been used to crosslink **P3HT**, with subsequent deposition and diffusion of **PCBM** affording 'structured bilayer' OPV devices delivering a 20% increase in PCE over the comparative bulk heterojunction [78]. In addition, whilst stability has not been assessed, such crosslinked **P3HT** films are insoluble permitting sequential layer deposition from the same solvent [79]. The structures of various crosslinkable small molecules are shown in Fig. 7.

The structurally similar bis-azide **Bis(PFBA)** has been used to crosslink an electron transport layer in an inverted OPV device, using just 10% weight (with respect to the polymer) and a DUV exposure time of five minutes to yield insoluble yet smooth films.

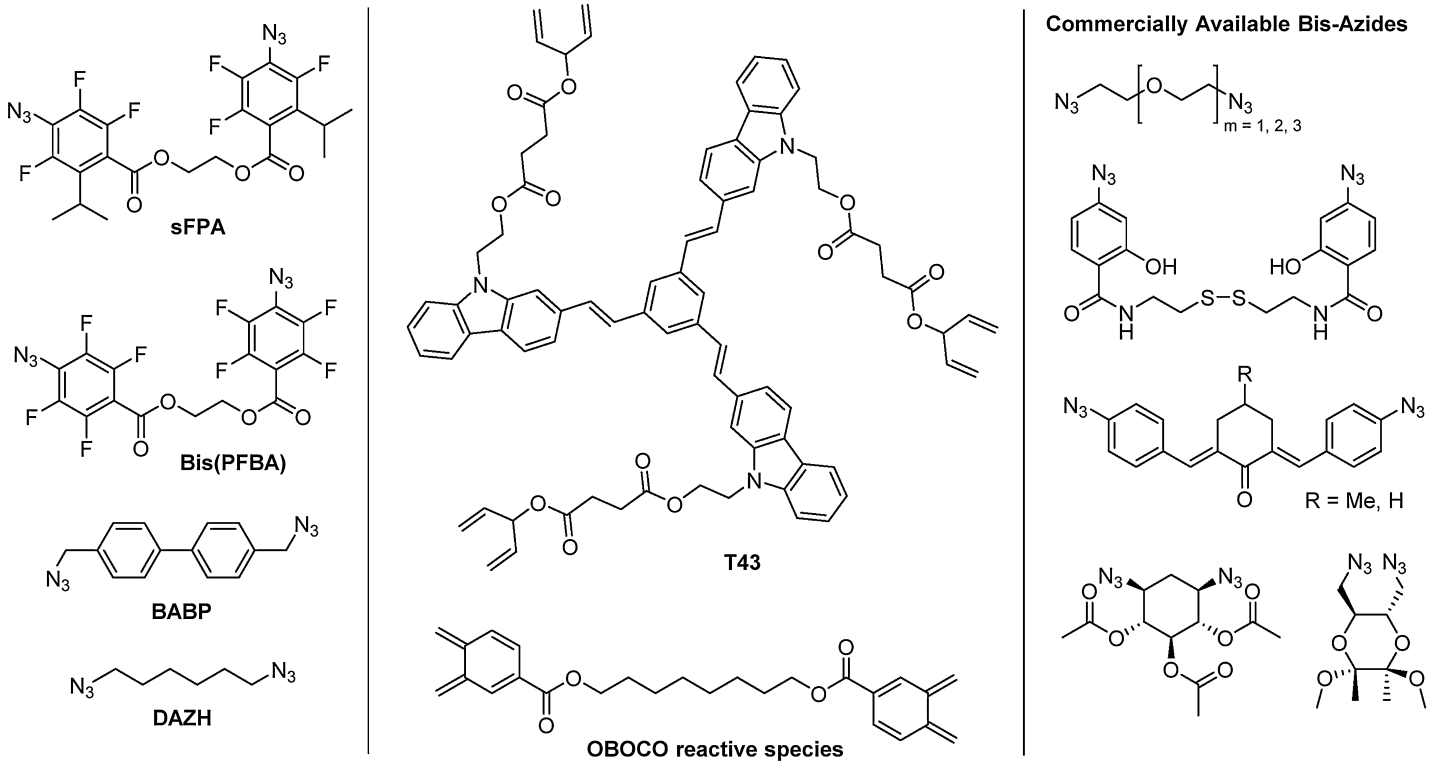

FIGURE 7

Crosslinkable small molecule additives.

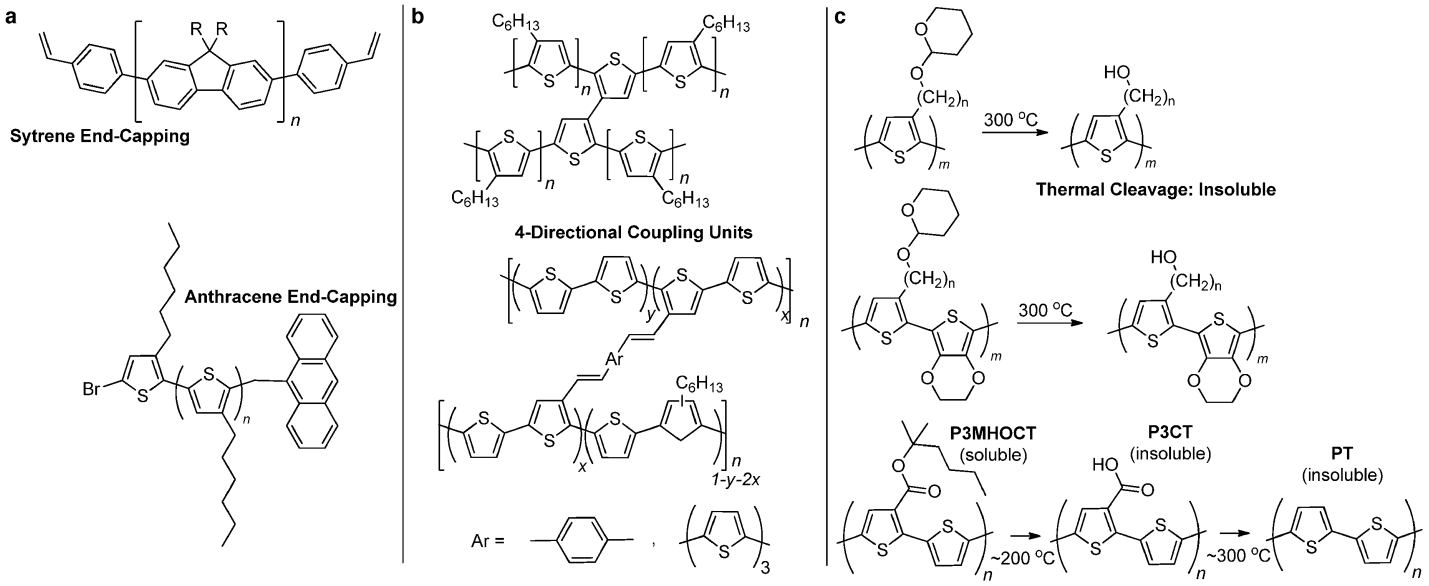

FIGURE 8

Alternative strategies to 'lock' morphology in organic semiconducting polymers.

The result was cells that retained an impressive 90% of their initial PCE (dropping from 3.4% to just 3.0%) after 20 days storage in air [80]. Bis-azide **BABP** has also been used, selectively crosslinking fullerenes on mild thermal activation in blends with either **P3HT**, **PTB7** or **PDPPTBT** to afford 60–90% retention of initial PCE on thermal ageing, depending on the polymer (see Table 2 for details). **BABP** is conveniently handled as a solid – unlike liquid **sFPA** – and can be used at just 2% weight addition with respect to the polymer [81].

We recently demonstrated that solid bis-azide **DAZH** could be used to crosslink **SiIDT-BT** acting as a dual-functional additive, boosting initial PCE from 6% to 7%. Moreover, after curing and thermal ageing the crosslinked device retained ~85% of initial PCE compared to <60% for the reference device. The improved stability is attributed to **DAZH** crosslinking frustrating fullerene aggregation and suppressing formation of a polymer layer at the cathode which, if instead allowed to build up, can block electron extraction leading to PCE decay [82]. Interestingly a number of bis-azides are available commercially which could potentially be used in a similar fashion, allowing for further work in this area (see Fig. 7).

The small molecule crosslinker concept is further demonstrated by **T43**, a photocrosslinkable leakage reducing buffer layer for incorporation in BHJ OPVs, increasing PCE. Moreover the use of an interlayer that can be insolubilized facilitates multi-layer devices without orthogonal solvent processing in a fashion that can be applied to large-scale printing methods [83]. Similarly, the use of azide-functionalized polymers with a tetra-propargyl ether containing small molecule additive has afforded sequential alignment

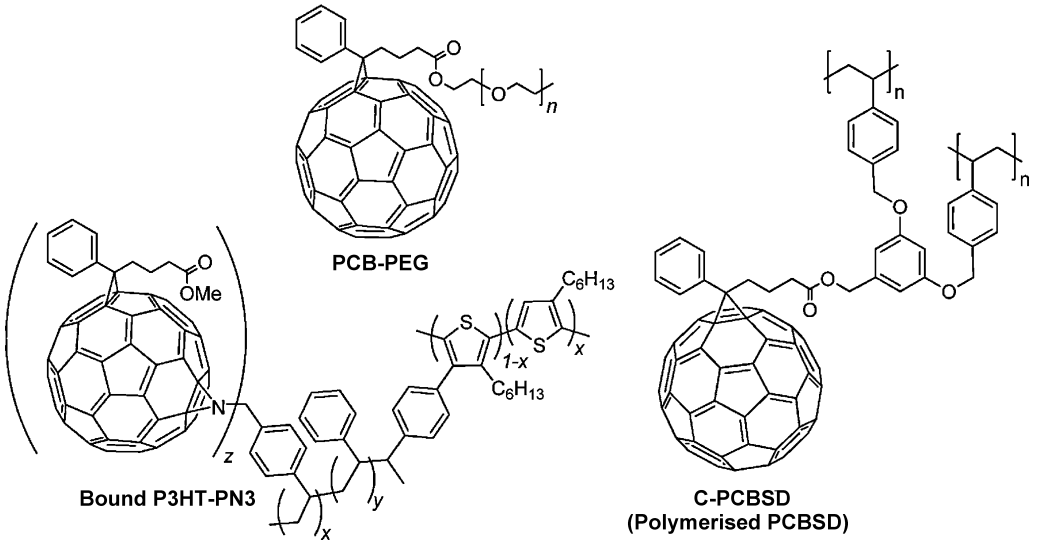

FIGURE 9

Functionalized fullerenes to 'lock' blend morphology.

and *in situ* crosslinking, resulting in long-term microstructure stability and very high optoelectronic activity at elevated temperatures (85°C), highlighting the wide range of materials and microstructures that can benefit from thermal stabilization by crosslinking [84].

More recently the molecule **OBOCO** has been developed. Upon thermal activation **OBOCO** undergoes a Diels–Alder reaction with fullerenes, effectively polymerizing them, exemplified by consistent hole mobility on thermal curing while electron mobility decreases in a blend with **P3HT**. While 5% weight **OBOCO** additive marginally improves PCE, using more than 5% weight reduces both fill-factor and short-circuit current density, reducing PCE. However, open-circuit voltage increases with **OBOCO** content up to 20% weight and is stable to ageing, conferring stability to the OPV cell, which retained 62% of its initial PCE on ageing at 150°C for 4 days, attributed to suppression of fullerene aggregation as determined by optical microscopy [63].

Alternative strategies to lock polymer morphology

A number of alternatives to those already discussed have also been proposed (see Fig. 8). For example the vinyl functionality has also been used to end-cap di-*n*-hexylfluorene and **P3HT** polymers, incorporated as either a styrene [85] or anthracene moiety [86]. The vinyl moieties are expected to react with fullerenes, which by optical microscopy inhibit aggregation, with initial PCE being largely independent of the UV exposure time.

Similarly, an alternative to crosslinking at the alkyl side-chains of polymers is to effectively build up polymers from 4-directional coupling units, which has also been exemplified with poly(thiophenes), bridged by either a single thiophene-to-thiophene covalent bond or a longer conjugated bridge [87]. However, in both these cases the direct binding to the conjugated backbone induces torsional twisting, reducing the conjugation length and decreasing PCE. Moreover, incorporating such 'bridged monomers' forms crosslinks prior to film deposition, rendering the polymers less soluble and hampering solution-processed deposition. While the use of longer, flexible aliphatic bridging units may alleviate the decrease in PCE by allowing free-rotation of the bridge without distorting the conjugated polymer backbone, the solubility of the polymer would remain encumbered.

Another alternative is to cleave the polymer's solubilizing groups *in situ*: for example the soluble polymer **P3MHOCT** undergoes

TABLE 2

Crosslinked OPV devices: initial performance and ageing comparison.

Crosslinker	Functionality	Reference PCE	Initial PCE	Aged PCE	PCE retention	Ageing regime
Polymers (w/PCBM)						
P3HNT	Vinyl	3.3%	3.2%	1.8%	56%	150°C, 10 h
P3HT-Br	Bromo	2.9%	2.6%	2.3%	88%	150°C, 48 h
P3HT-N5[a]	Azide	2.2%	1.5%	1.0%	67%	110°C, 40 h
TQ-Bromo[b]	Bromo	1.5%	1.8%	–	~50%	rt, 45 h, constant illumination
TQ-Oxetane[b]	Oxetane		1.2%	–	–	
TQ-Vinyl[b]	Vinyl		1.6%	–	~30%	
TQ-Azide[b]	Azide		1.2%	–	~45%	
PBT-Br	Bromo	2.7%	2.7%	2.1%	78%	150°C, 80 h
PBT-N_3	Azide		2.6%	1.8%	69%	
PBT-Vinyl	Vinyl		2.6%	1.3%	50%	
PBDTTPD	Bromo	5.2%	3.3%	4.6%	139%	150°C, 72 h
PBDTTT-Br25	Bromo	4.3%	5.2%	3.4%	65%	150°C, 24 h
PCPDT-TBTT-Vinyl	Vinyl	–	1.4%	1.1%	79%	200 h, ambient
PBbTTT-TT	Bromo	–	2.6%	2.4%	92%	150°C, 40 h
Additives						
sFPA (w/P3HT/PCBM)[c]	Azide	3.3%	3.0%	–	–	–
Bis(PFBA) (w/P3HT/PCBM)[d]	Azide	–	3.4%	3.0%	88%	rt, 20 days in air
BABP (w/P3HT/PCBM)	Azide	3.3%	3.3%	3.0%	90%	85°C, 120 days
BABP (w/PTB7/PCBM)	Azide	5.4%	–	4.6%	85%	150°C, 16 h
BABP (w/PDPPTBT/PCBM)	Azide	5.0%	–	3.0%	60%	150°C, 15 h
DAZH (w/SiIDT-BT/PCBM)	Azide	6.0%	7.0%[g]	4.1%	82%	85°C, 14 h
OBOCO (w/P3HT:PCBM)	Vinyl	2.7%	2.8%	1.7%	61%	150°C, 4 days
Fullerenes						
C-PCBSD (w/P3HT)	Vinyl	4.1%	3.3%	3.7%	112%	150°C, 25 h
C-PCBS (w/P3HT)	Vinyl		3.8%	3.6%	95%	
C-PCBSD[e] (w/P3HT:PCBM)	Vinyl	3.5%	4.4%	3.8%	86%	rt, 35 days, unencapsulated in air
P3HT-PN3	Azide	2.5%	1.8%	0.6%	33%	150°C, 5 h
PCB-PEG/Cu[f] (w/P3HT:PCBM)	–	3.6%	2.2%	1.8%	82%	15 days

Reference values are for the non-crosslinked and non-functionalized analogue polymers. All fabrication, measurements and ageing assumed to be under an inert atmosphere unless stated otherwise.

[a] Ambient fabrication.

[b] With an inverted device architecture and silver electrode (ITO/ZnO/polymer:fullerene/PEDOT:PSS/Ag).

[c] Structured bilayer.

[d] Used to crosslink an electron transport layer in an inverted device.

[e] Used as an interlayer.

[f] Used as an electrode in a P3HT:PCBM blend.

[g] The post-curing PCE was 5.7% (prior to ageing).

thermal treatment at ~200°C then ~300°C to afford insoluble poly(thiophene). However, this also reduces PCE [88].

Fullerene-based crosslinking strategies

The use of crosslinkable and immobilized fullerene-derived electron acceptor materials has also been studied (see Fig. 9). One approach is to polymerize the fullerenes *in situ*, for example bis-styryl **PCBSD** [89], resulting in a highly inter-locked network on thermal annealing in a blend with **P3HT** (180°C for 30 min). A PCE of ~3.7% was achieved after ageing (150°C for 25 h) being higher than the as-made value of ~3.3%. Furthermore, similar performance and stability was observed when using the mono-styryl analogue **PCBS** (3.7–3.6% PCE over the same ageing regime), with an optimized weight ratio of 6:5:1 **P3HT/PCBM/Functionalized-PCBM**. Whilst initial performance was lowered in both cases, stability was greatly improved compared to the reference (which decreased from 4.1% to 0.7%), being attributable to immobilization of the fullerenes, thus suppressing crystallization [62].

Instead of polymerizing the fullerene directly, it is also possible to functionalize the polymer with well-spaced crosslinking groups that can selectively bind, as demonstrated with **P3HT-PN3**, which uses an azide and poly(phenylethylene) spacer grafted onto 1% of **P3HT** repeat units. However, π-binding of the azide to the fullerene lowered the initial PCE by ~0.7% and the deterioration of PCE over time was only marginally suppressed [90].

Alternatively, functionalized fullerenes can be used as processing additives to improve stability: the addition of 5% by weight **PCB-PEG** leads to a spontaneous vertical phase separation and formation of a covering protective monolayer which both improves thermal stability and efficiency. PCE rises in comparison to the reference **P3HT:PCBM** device by 0.8% (from 3.6% to 4.4%) with a high voltage, current and fill-factor in optimized devices. In addition, whilst initial PCE is reduced, with a copper electrode 80% is retained after 360 h, compared to just 20% with an aluminium electrode, serving as a promising example of additional device enhancement [91].

Crosslinked OPV devices summary table

The initial and aged performance of the various crosslinked OPV devices described above are summarized in Table 2.

Conclusions and outlook

In summary, state-of-the-art crosslinking strategies utilize UV or thermal treatment that have demonstrated the potential to be incorporated into large-scale solution processed manufacturing methods. Crosslinks are desirably formed at locations which don't perturb the conjugated system of both components and critical microstructure of the active blend. This is optimally between the termini of solubilizing alkyl side-chains, *via* either attached functional groups (bromo/oxetane/vinyl/azide) or selective small molecule crosslinkers (2-, 3- or 4-D coupling units) which may be added to a blend solution. To-date the bromo functionality typically confers the greatest stability. It is often necessary to perform crosslinking under an inert atmosphere (to avoid photo-oxidation) and this could densify the polymer network improving packing and solid state interactions, boosting short-circuit current and thus initial PCE but at the risk of electrode delamination. Alternative approaches have lower crosslinking densities, require harsh heat treatments and can encumber device efficiency, or involve expensive fullerene derivatives. However, these important research fields require further study and optimization.

While functionalized polymers may be more readily characterized, the use of multi-directional (>2D) crosslinking small molecule additives is of interest due to their greater versatility, as well as optimization of existing materials processing and synthesis.

References

[1] Chemistry Nobel Prize 2000.
[2] M. Pagliaro, G. Palmisano, R. Ciriminna, Flexible Solar Cells, Wiley-VCH, Weinheim, 2008.
[3] J. Rivnay, R.M. Owens, G.G. Malliaras, Chem. Mater. 26 (2014) 679.
[4] BASF, BASF Chemistry World Tour Innovations, 2013.
[5] G. Dennler, M.C. Scharber, C.J. Brabec, Adv. Mater. 21 (2009) 1323.
[6] A. Facchetti, Chem. Mater. 23 (2011) 733.
[7] H. Zhou, L. Yang, W. You, Macromolecules 45 (2012) 607.
[8] T.D. Nielsen, et al. Sol. Energy Mater. Sol. Cells 94 (2010) 1553.
[9] Mitsubishi Chemical Corporation No Title.
[10] J. You, et al. Nat. Commun. 4 (2013) 1446.
[11] J. You, et al. Adv. Mater. (Deerfield Beach, Fla.) 25 (2013) 3973.
[12] C.J. Brabec, et al. Adv. Mater. 22 (2010) 3839.
[13] M. Jørgensen, et al. Adv. Mater. (Deerfield Beach, Fla.) 24 (2012) 580.
[14] J. Ahmad, et al. Renew. Sust. Energy Rev. 27 (2013) 104.
[15] J.U. Lee, et al. J. Mater. Chem. 22 (2012) 24265.
[16] L. Dou, et al. Adv. Mater. (Deerfield Beach, Fla.) 25 (2013) 6642.
[17] H.J. Son, et al. Energy Environ. Sci. 5 (2012) 8158.
[18] A.J. Heeger, Adv. Mater. (Deerfield Beach, Fla.) 26 (2014) 10.
[19] C.L. Chocos, S.A. Choulis, Prog. Polym. Sci. 36 (2011) 1326.
[20] M.T. Dang, et al. Chem. Rev. 133 (2013) 3734.
[21] P.P. Khlyabich, et al. Polymer (2013).
[22] W. Ma, et al. Adv. Funct. Mater. 15 (2005) 1617.
[23] L. Lu, L. Yu, Adv. Mater. (2014).
[24] Z. He, et al. Nat. Photon. 9 (2015) 174.
[25] P. Liu, et al. Chem. Mater. (2014).
[26] C. Cabanetos, et al. J. Am. Chem. Soc. 135 (2013) 4656.
[27] X. Hu, et al. Adv. Energy Mater. (2014).
[28] X. Guo, et al. Nat. Photon. 7 (2013) 825.
[29] K.-S. Chen, et al. Adv. Mater. (2014).
[30] R.S. Ashraf, et al. J. Am. Chem. Soc. 137 (2015) 1314.
[31] Y. Liu, et al. Nat. Commun. 5 (2014) 5293.
[32] J. You, et al. Prog. Polym. Sci. 38 (2013) 1909.
[33] W. Li, et al. J. Am. Chem. Soc. 135 (2013) 5529.
[34] L.T. Dou, et al. Nat. Photon. 6 (2012) 180.
[35] L. Dou, et al. J. Am. Chem. Soc. 134 (2012) 10071.
[36] L.T. Dou, et al. Adv. Mater. 25 (2013) 825.
[37] K. Li, et al. J. Am. Chem. Soc. 135 (2013) 13549.
[38] J. You, et al. Adv. Mater. 25 (2013) 3973.
[39] J.B. You, et al. Nat. Commun. 4 (2013) 1446.
[40] A. Mishra, P. Bauerle, Angew. Chem. Int. Ed. 51 (2012) 2020.
[41] M. Riede, et al. Adv. Funct. Mater. 21 (2011) 3019.
[42] A. Facchetti, Mater. Today 16 (2013) 123.
[43] P.D. Topham, A.J. Parnell, R.C. Hiorns, J. Polym. Sci. B: Polym. Phys. 49 (2011) 1131.
[44] P. Sonar, J.P.F. Lim, K.L. Chan, Energy Environ. Sci. 4 (2011) 1558.
[45] A.F. Eftaiha, et al. J. Mater. Chem. A 2 (2014) 1201.
[46] S. Holliday, et al. J. Am. Chem. Soc. 137 (2015) 898.
[47] C.B. Nielsen, et al. Adv. Mater. 27 (2015) 948.
[48] M.J. Robb, et al. J. Polym. Sci. A: Polym. Chem. 51 (2013) 1263.
[49] J. Rivnay, et al. Chem. Rev. 112 (2012) 5488.
[50] R. Noriega, et al. Nat. Mater. 12 (2013) 1038.
[51] M.-S. Kim, et al. Appl. Phys. Lett. 90 (2007) 123113.
[52] N. Haberkorn, S.A.L. Weber, P. Theato, ACS Appl. Mater. Interfaces 2 (2010) 1573.
[53] N. Haberkorn, et al. Macromol. Chem. Phys. 212 (2011) 2142.
[54] J. Peet, et al. Nat. Mater. 6 (2007) 497–500.
[55] H. Kim, W.-W. So, S.-J. Moon, J. Kor. Phys. Soc. 48 (2006) 441.
[56] S.M. Lindner, et al. Angew. Chem. Int. Ed. 45 (2006) 3364.
[57] C. Goh, K.M. Coakley, M.D. McGehee, Nano Lett. 5 (2005) 1545.
[58] H.J. Snaith, et al. Nano Lett. 5 (2005) 1653.

[59] M. Jørgensen, et al. Adv. Mater. 24 (2012) 580.
[60] S. Cros, et al. Sol. Energy Mater. Sol. Cells 95 (2011) 865.
[61] G. Griffini, et al. Adv. Mater. (Deerfield Beach, Fla.) 23 (2011) 1660–1664.
[62] Y.-J. Cheng, et al. Adv. Funct. Mater. 21 (2011) 1723.
[63] D. He, et al. J. Mater. Chem. A 1 (2013) 4589.
[64] K. Lu, et al. Macromolecules 42 (2009) 3222.
[65] B.J. Kim, et al. Adv. Funct. Mater. 19 (2009) 2273.
[66] S. Miyanishi, K. Tajima, K. Hashimoto, Macromolecules 42 (2009) 1610.
[67] C.-Y. Nam, et al. Macromolecules 45 (2012) 2338.
[68] F. Piersimoni, et al. J. Polym. Sci. B: Polym. Phys. 51 (2013) 1209.
[69] Z. Li, et al. Nat. Commun. 4 (2013) 2227.
[70] S. Feser, K. Meerholz, Chem. Mater. 23 (2011) 5001.
[71] B.A.G. Hammer, et al. ACS Appl. Mater. Interfaces 6 (2014) 7705.
[72] J.E. Carlé, et al. J. Mater. Chem. 22 (2012) 24417.
[73] X. Chen, L. Chen, Y. Chen, J. Polym. Sci. A: Polym. Chem. 51 (2013) 4515.
[74] Y. Liang, et al. Adv. Mater. 22 (2010) E135.
[75] D. Qian, et al. J. Polym. Sci. A: Polym. Chem. 51 (2013) 3123.
[76] K. Yao, et al. Org. Electron. 13 (2012) 1443.
[77] R.-Q. Png, et al. Nat. Mater. 9 (2010) 152.
[78] B. Liu, et al. Nat. Commun. 3 (2012) 1321.
[79] C. Tao, et al. Adv. Energy Mater. 3 (2013) 105.
[80] N. Cho, et al. Adv. Energy Mater. 1 (2011) 1148.
[81] L. Derue, et al. Adv. Mater. 26 (2014) 5831.
[82] J.W. Rumer, et al. Adv. Energy Mater. (2015).
[83] N. Su Kang, et al. Sol. Energy Mater. Sol. Cells 95 (2011) 2831.
[84] Z. Shi, et al. ACS Macro Lett. 1 (2012) 793.
[85] G. Klärner, et al. Chem. Mater. 11 (1999) 1800.
[86] S. Khiev, et al. Polym. Chem. 4 (2013) 4145.
[87] E. Zhou, et al. Macromolecules 40 (2007) 1831.
[88] J.L. Brusso, M.R. Lilliedal, S. Holdcroft, Polym. Chem. 2 (2011) 175.
[89] C.-H. Hsieh, et al. J. Am. Chem. Soc. 132 (2010) 4887.
[90] B. Gholomkhass, S. Holdcroft, Chem. Mater. 22 (2010) 5371.
[91] J.W. Jung, J.W. Jo, W.H. Jo, Adv. Mater. 23 (2011) 1782.